Carbohydrate Polymers 94 (2013) 765–772

Contents lists available at SciVerse ScienceDirect

Carbohydrate Polymers

journal homepage: www.elsevier.com/locate/carbpol

Influence of citric acid and curing on moisture sorption, diffusion and permeability of starch films

Erik Olsson[a,*], Mikael S. Hedenqvist[b], Caisa Johansson[a], Lars Järnström[a]

[a] Department of Chemical Engineering, Karlstad University, SE-651 88 Karlstad, Sweden
[b] Fibre and Polymer Technology, Royal Institute of Technology, SE-100 44 Stockholm, Sweden

ARTICLE INFO

Article history:
Received 28 June 2012
Received in revised form 29 January 2013
Accepted 5 February 2013
Available online 20 February 2013

Keywords:
Starch
Citric acid
Cross-linking
Diffusion
Moisture content
Permeability

ABSTRACT

Starch films with different amounts of citric acid produced by solution casting were subjected to different curing temperatures and compared with films plasticized with glycerol. The films were tested in a controlled moisture generator, which enabled the moisture sorption to be measured and the diffusion coefficient and water vapor permeability to be calculated. It was shown that increasing the amount of citric acid added led to a reduction in the equilibrium moisture content, diffusion coefficient and water vapor permeability of the films, the values of which were all considerably lower than the values obtained for the films plasticized by glycerol. It was also seen that curing the film with 30 pph citric acid at 150 °C led to a significant reduction in the equilibrium moisture content, the diffusion coefficient and the water vapor permeability at high relative humidity which suggests that crosslinking occurred. The calculated water vapor permeability data were comparable with the value obtained with direct measurements.

1. Introduction

The replacement of synthetic polymers with renewable materials as barriers for consumer packages is an ongoing research topic. One candidate is thermoplastic starch, TPS, a renewable and fully biodegradable material. However, one of the main problems associated with TPS is its inherent sensitivity to water due to the hydrophilic and hygroscopic nature of starch and its plasticizers and the high plasticizing power of water (Mathew & Dufresne, 2002). It has been observed that the TPS barrier properties are significantly reduced with increasing relative humidity, RH (Gaudin, Lourdin, Forssell, & Colonna, 2000) or when the moisture content reaches a critical value (Forssell, Lahtinen, Lahelin, & Myllarinen, 2002). Water activity is an important factor for microbial growth and food texture and the provision of a barrier against water is thus a major concern in food packaging. Recent research on how to better utilize TPS as a barrier involves strategies to minimize this water sensitivity such as blending with a synthetic polymer (Ning, Xingxiang, Na, & Jianming, 2010; Shi et al., 2008) or a natural polymer (Gaspar, Benko, Dogossy, Reczey, & Czigany, 2005), the incorporation of inorganic fillers such as clay (Magalhães & Andrade, 2009; Park et al., 2003), the incorporation of organic fillers based on cellulose (Averous, Fringant, & Moro, 2001; Lopez-Rubio et al., 2007; Svagan, Hedenqvist, & Berglund, 2009) or starch (Angellier, Molina-Boisseau, Dole, & Dufresne, 2006; Habibi & Dufresne, 2008), modifying the starch (Jansson & Jarnstrom, 2005; Jonhed, Andersson, & Jarnstrom, 2008; Yu, Chang, & Ma, 2010), utilizing different plasticizers (Huang, Yu, & Ma, 2006; Lourdin, Coignard, et al., 1997), using co-plasticizers (Shi et al., 2007) and cross-linking the starch (Seidel et al., 2001; Yoon, Chough, & Park, 2006).

The addition of citric acid (CA) to renewable barrier materials has been the subject of recent publications due to the potential of CA to enhance both the mechanical and barrier properties. CA is a naturally occurring polycarboxylic acid present in fruits such as lemon and lime. CA is biodegradable and renewable and is generally classified as safe for food usage and is included in many food products such as jams, juices and soft drinks. CA has been shown to affect TPS in several intriguing ways. CA has been shown to cross-link polysaccharide materials such as starch granules (Xie & Liu, 2004), starch nano-particles (Ma, Jian, Chang, & Yu, 2008), TPS (Jiugao, Ning, & Xiaofei, 2005; Reddy & Yang, 2010), cotton fibers (Blanchard, Reinhardt, Graves, & Andrews, 1994), xylan films (Talja & Poppius-Levlin, 2010), chitosan (Moller, Grelier, Pardon, & Coma, 2004) and hydroxypropyl cellulose films (Coma, Sebti, Pardon, Pichavant, & Deschamps, 2003). CA also acts as a plasticizer (Shi et al., 2007) and has been shown to promote starch hydrolysis by lowering the pH (Hirashima, Takahashi, & Nishinari, 2004; Shi et al., 2007).

* Corresponding author. Tel.: +46 54 7002172; fax: +46 54 7002040.
E-mail address: erik.olsson@kau.se (E. Olsson).

0144-8617/$ – see front matter © 2013 Elsevier Ltd. All rights reserved.
http://dx.doi.org/10.1016/j.carbpol.2013.02.006

Starch has the potential to be cross-linked by poly-functional reagents which are able to react with two or more of the hydroxyl groups. The cross-links can be either intramolecular, within the same polymer chain or intermolecular, between different polymer chains. Intermolecular cross-linking reactions increase the average molecular weight of the starch (Rutenberg & Solarek, 1984) and introduces chemical bridges between different molecules, which reduces the swelling in liquid water or at high RH. The swelling tendency decreases with increasing number of cross-links (Wurzburg, 1986). Cross-linking of TPS is a potential method of improving its barrier properties by reducing the moisture content and minimizing the molecular movement and hence reducing the diffusion of small molecules through the film. Typical cross-linkers for TPS include dichloroacetic acid (He et al., 2007), phosphorus oxychloride (Wang & Wang, 2000), sodium trimetaphosphate (Deetae et al., 2008), epichlorohydrin (Lelievre, 1984), calcium hydroxide, zirconium acetate (Shogren, Lawton, Tiefenbacher, & Chen, 1998), glutaraldehyde (Yoon, Chough, & Park, 2006) and various polycarboxylic acids (Seidel et al., 2001). Another route is to modify the starch into a more reactive form like dialdehyde starch (Yu, Chang, & Ma, 2010). One advantage of using CA as a cross-linker in food packaging applications is that unreacted CA remnants are considered to be nutritionally harmless and that they act as a plasticizer for TPS (Shi et al., 2008).

Hydrolysis, leading to a reduction in the starch molecular weight at low pH and elevated temperature is however reported to be the predominant reaction between starch and CA at high moisture content (Shi et al., 2007). Some processes in which hydrolysis of starch with CA have been shown to occur are melt processing in the presence of sufficient amounts of water (Carvalho, Zambon, Da Silva Curvelo, & Gandini, 2005), gelatinization (Hirashima et al., 2004) and drying (Wing, 1996). Wing (1996) reports that if the films are dried at a low temperature, in order to remove most of the water before curing where the cross-linking reaction occurs, a higher reaction efficiency without excessive hydrolysis can be achieved, resulting in a higher molecular weight (Wing, 1996).

Molecular transport through a polymer film occurs mainly through defects in the film such as cracks, voids and pinholes where the gas molecules have free passage through the film or by diffusion through the amorphous regions (Andersson, 2008). The addition of a plasticizers such as glycerol (GLY) (Forssell et al., 2002; Stading, Rindlav-Westling, & Gatenholm, 2001), sorbitol (Lourdin, Coignard, et al., 1997; Mali, Sakanaka, Yamashita, & Grossmann, 2005), fructose (Kalichevsky & Blanshard, 1993), xylitol (Chaudhary & Adhikari, 2010) or poly-ethylene glycol (Lourdin, Coignard, et al., 1997) reduces the glass transition temperature, T_g, of the polymer matrix and helps to avoid the formation of cracks and pinholes. Not only the type of plasticizer but also the ratio of plasticizer to starch is important for the plasticization. Diffusion through the amorphous regions is due to gas molecules jumping between neighboring free volume holes. In general, the permeability of a solute through a phase is dependent on the product of the amount of solute in the phase, its solubility, and the rate at which transport occurs, its diffusion coefficient (Crank, 1975):

$$P = D \times S \quad (1)$$

where P is the permeability coefficient, D is the diffusion coefficient and S is the solubility.

It has been shown that a plasticizer like GLY tends to have a dual effect on the moisture sorption in TPS. At low RH and low plasticizer content, the plasticizer tends to decrease the moisture sorption which has been explained as being due to a competition for the polar interaction sites on starch between the plasticizer and water (Godbillot, Dole, Joly, Roge, & Mathlouthi, 2006). This tends to reduce the movement of both the plasticizer and the polymer chains, so that the polymer becomes more rigid (Cadogan & Howick, 2008). This is called antiplasticization and is known to result in reduced mobility and more brittle materials. For instance, for GLY-plasticized TPS, there is a critical GLY content below 12 wt% at which antiplasticization occurs (Lourdin, Bizot, & Colonna, 1997a). At high plasticizer content and high RH, when the polymer sorption sites are saturated with plasticizer, the plasticizer tends to increase the moisture sorption. This has been explained in terms of a phase-separation phenomenon into starch-rich and plasticizer-rich phases where the water is preferably absorbed by the plasticizer-rich phase (Godbillot et al., 2006). For a starch–GLY–water system, T_g measurements have shown that there is a phase transition into starch-rich and plasticizer-rich regions when the plasticizer content is increased. This behavior is not specific for GLY and water but has also been shown to occur with fructose (Kalichevsky & Blanshard, 1993) and sorbitol (Gaudin, Lourdin, Le Botlan, Ilari, & Colonna, 1999). The phase-separation behavior is very important for the plasticizing mechanism. It has been reported elsewhere that the plasticizing effect of GLY is not due to the formation of a rubbery phase but rather due to clustering of plasticizer-rich areas (Gaudin et al., 1999).

The aim of the present work was to study how the diffusivity and solubility of TPS are affected by CA at different plasticizer concentrations and different curing temperatures and how this affects the water vapor permeability, WVP. A comparison was also made with GLY, the most widely used plasticizer for TPS, as reported in the literature.

2. Materials and methods

2.1. Materials

2.1.1. Starch

A hydroxypropylated and oxidized potato starch (Solcoat 155) was supplied by Solam (Kristianstad Sweden). The starch had an amylose content of 21%, a degree of substitution of hydroxypropyl groups of 0.11, an average 0.01 carboxyl groups of per anhydroglycose unit (Jonhed et al., 2008) and a viscosity of 180 cP at 20% solids content, Brookfield LVDV 100 rpm, and 50 °C, for jet cooked starch according to the supplier.

2.1.2. Additives

CA and GLY was used as plasticizers. Both CA, anhydrous citric acid puriss and GLY, glycerol reagent plus (R) were purchased from Sigma–Aldrich Inc., St. Louis, MO, USA.

2.2. Methods

2.2.1. Starch gelatinization

The starch solution was prepared by dispersing approximately 25 g of dry starch (50 g in the case of the coated paper) in deionized water to a total weight of 250 g. The aqueous starch dispersion was gelatinized by immersion in a boiling water bath under vigorous stirring for 45 min. Since the addition of CA to starch can cause hydrolysis at high temperature and high water content, CA was added after the gelatinization. The same procedure was used when GLY was added. Addition of CA at concentrations from 5 to 30 pph resulted in pH ranging from 1.9 to 2.5 in the starch solution.

2.2.2. Preparation of free films

Films were cast by pouring 10.0 ± 0.1 g of the starch–plasticizer solution into 88 mm diameter polystyrene Petri dishes followed by drying at 70 °C in a self-ventilated oven for 5 h, in order to remove most of the water at low temperature to prevent unwanted hydrolysis. The films were prepared without plasticizers, with 5, 10, 20 and 30 parts (by wt) per hundred parts of dry starch (pph) CA, 30 pph GLY and a combination of 5 pph CA and 30 pph GLY. The

dried films were placed in desiccators over dry silica gel for 24 h at room temperature. For the high temperature curing at 105 °C, 130 °C (for 30 pph CA only) and 150 °C, the dried samples were removed from the Petri dishes and placed on aluminum foil for 10 min in a non-ventilated oven at the desired curing temperature. All films were equilibrated at 23 °C and 50% RH for at least 1 week before further investigation. The moisture content of the films equilibrated at 23 °C 50% RH was determined in at least triplicates to provide a reference for the investigation of the moisture uptake. These films were cut into small pieces, approx 0.1 g, and were weighed and dried in an oven at 105 °C for 1 h. The experimental data from these films were statistically analyzed by ANOVA and the *F*-test.

2.2.3. Preparation of coated paper

Coated paper was used in this study since it was easier to handle than free films in the measurements of Mocon WVTR. Super Perga WS Parchment (Nordic Paper Säffle, Sweden) was used as paper substrate and the papers were coated on a bench coater (K202 Control Coater, RK Coat Instruments Ltd., Royston, UK). The coating was applied in two layers with a wire-wound bar, 0.15 mm wire diameter, at speed 4 resulting in a total coat weight of 10 g/m^2. The coating consisted of 100 pph starch with 30 pph CA, with a drying temperature of 70 °C for 90 s after application of each coating layer, followed by 1 h of post-drying at 70 °C in order to simulate the conditions of the dried films.

2.2.4. Thickness of free films

The actual thickness of the films as a function of time could not be measured directly during the experiment. Neither was it possible to find one method which worked to measure the thickness for all the samples before the moisture sorption trials. Some samples were brittle and cracked during measurement and some were soft and deformed. Therefore, the thicknesses were estimated from separately performed density measurements. The increase in film thickness due to the absorption of water was calculated using the fractional thickness change, which is an approximation assuming that the volumes of water and matrix are additive (Cho, Gällstedt, & Hedenqvist, 2010):

$$\frac{d_a}{d_i} = \left[1 + \frac{w_\infty(1-w_n)}{(\rho_2/\rho_1) - w_\infty(1+w_n) + w_\infty^2 W_n(\rho_1/\rho_2)}\right]^{-1/3} \quad (2)$$

where d_a is the actual thickness, d_i is the calculated thickness at 90% RH, w_∞ is the weight fraction of water at 90% RH, w_n is the normalized weight fraction of water(with respect to the weight fraction of water at 90% RH), and ρ_1 and ρ_2 are the densities of water and of the starch/non-volatile plasticizer phase, respectively.

The density of the dry films was determined by Archimedes principle on a Precisa Density Determinations Kit connected to a Precisa 410AM-FR analytical scale (Precisa Gravimetrics AG, Dietlikon, Switzerland) by immersing the films in octane. All measurements were performed at least in triplicate. The films were dried at 23 °C in desiccators with silica gel for 120 h before the density determinations.

2.2.5. Moisture uptake

For the moisture uptake, a Controlled Moisture Generator, CMG (TJT-Teknik AB, Järfälla, Sweden) was used. The weight of the sample was recorded on an analytical balance. The temperature inside the chamber was set to 23 °C. The chamber conditions were monitored every minute during the testing sequence.

Before the sorption trials were performed, the TPS films were conditioned in a room with controlled temperature and RH conditions (23 °C and ~25% RH) for at least 3 days. The RH in the controlled moisture generator was increased in steps from 50–60–70–80–90% RH at set time intervals in order to obtain moisture sorption isotherms and diffusion coefficients. The diffusion coefficient was assumed to be independent on the moisture content within each step. The dry weight of the films was determined gravimetrically by drying the films in a well-ventilated oven at 105 °C overnight after the sorption experiments. The samples were thin films, 88 mm in diameter and the thickness varied between 150 and 250 μm depending on the recipe and surrounding RH. The sorption experiments were performed in single replicates with the exception of the non-cured 30 pph CA films that were performed in triplicate to give an estimate of the uncertainty. The data were statistically analyzed with linear regression analysis and Student's *t*-test with respect to the non-cured 30 pph CA sample. For comparison, the moisture uptake of crystalline anhydrous CA powder was also measured.

For the films that had not reached an equilibrium weight at the end of each sequence, the equilibrium weight uptake was determined by fitting the experimental data points to the equation.

$$\frac{t}{m_t} = \frac{t}{m_\infty} + \frac{1}{Km_\infty} \quad (3)$$

where t is the time, m_t is the weight uptake at the time t, m_∞ is the weight uptake at time infinity and K is a constant. Eq. (3) was arbitrarily selected as an equation where m_t asymptotically approaches m_∞ as t goes toward infinity, with m_∞ and K as the fitting parameters.

Diffusion with a concentration-dependent diffusion coefficient into a film is described by Fick's second law (Crank, 1975):

$$\frac{dC}{dt} = \frac{d}{dx}\left[D(C)\frac{dC}{dx}\right] \quad (4)$$

where t is the time, C is the permeant concentration and x is the distance along the sample thickness.

The diffusion coefficients were determined by two different methods based on the analytical solution of Fick's first law (Crank, 1975) here referred to as method 1* and method 2*. Method 1* (Eq. (5)) gives the diffusion coefficient from the time it takes to reach half of the equilibrium uptake, and method 2* (Eq. (6)) gives the diffusion coefficient from the shape of the latter part of the sorption curve. Both methods assume uni-dimensional diffusion, a constant diffusion coefficient, no swelling, equilibrium moisture content at the surface and no moisture gradient at the start of each change in RH (Crank, 1975).

$$D = 0.0419/(t_{0.5}/L^2) \quad (5)$$

$$\ln\left(1 - \frac{M_t}{M_{eq}}\right) = \ln\frac{8}{\pi^2} - \frac{\pi^2 Dt}{L^2} \quad (6)$$

where $t_{0.5}$ is the time to reach half the equilibrium moisture uptake, L is the thickness (half of the film thickness due to symmetry), M_t is the mass uptake at time t and M_{eq} is the mass uptake at equilibrium.

2.2.6. Permeability of coated paper

The water vapor transmission rate, WVTR was measured in duplicate using a Mocon Permatran-W 3/33 (MOCON, Inc., Minneapolis, USA) according to ISO 9932:1990(E) at 23 °C. The measurements were performed as a gradient series across coated paper with an area of 5 cm^2. The series consisted of: 50-0, 60-0, 70-0, 80-0 and 90-0% RH and was performed from low to high RH. Before the measurements, the specimens were conditioned at the measurement conditions with 50–90% RH on one side and dry nitrogen gas on the other until equilibrium was achieved. The water vapor permeability, WVP(*Dir*) was calculated from the WVTR results according to:

$$WVP(Dir) = \frac{WVTR \times h}{p \times (R_1 - R_2)} \quad (7)$$

Table 1
Mean density and standard deviation for the different recipes without embedded air bubbles. These values were used in the calculation of film thickness according to Eq. (2).

Recipe	Density (g/cm^3)
0 CA	1.45 ± 0.07
5 CA	1.49 ± 0.04
10 CA	1.48 ± 0.05
20 CA	1.43 ± 0.10
30 CA	1.44 ± 0.13
30 GLY	1.49 ± 0.02
5 CA 30 GLY	1.46 ± 0.05

WVP(*Calc*) the was calculated from the diffusion and solubility data according to:

$$WVP(Calc) = \frac{D \times S}{p \times (R_1 - R_2)} \quad (8)$$

where h is the thickness of the coating layer, p is the partial pressure of water, R_1 and R_2 are the relative humidity on the high and low RH side of the specimen respectively, D is the diffusion coefficient and S is the solubility. The thickness was calculated from the coat weight and the density of the coating.

In this comparison, some simplifications were made. In reality, the permeability of the coated paper is dependent on the thickness of the coating layer, the paper and the amount of coating that has filled the pores of the paper. The influence of the paper on the WVP was however neglected and the permeability was calculated considering only the coating layer in which the diffusion path length was assumed to be uniform for the given thickness. This was done in order to compare the permeability values calculated from the diffusion coefficient and solubility with the directly measured permeabilities. The WVP calculated from the diffusion coefficient and solubility at a given RH was compared with the WVP from the gradient between the actual RH and 0% RH.

3. Results and discussion

3.1. Thickness of films: density determinations

The average densities of the dried TPS films with CA and GLY are shown in Table 1. In the density determinations, the films cured at 150 °C with more than 20 pph CA or with 30 pph GLY had a significantly lower density and showed a greater scatter in data than the other samples (data not shown). This was due to embedded air-bubbles non-uniformly distributed in the films. These films were therefore excluded when the average density was calculated. The table shows data from at least 8 measurements. Due to the relatively high standard deviation of these measurements it was not possible to draw any clear conclusions from the density changes with increasing CA content or differences between CA and glycerol. These density determinations made it possible to estimate the thickness at each relative humidity with Eq. (2). The calculated thickness of the films varied from approximately 150 to 220 μm.

3.2. Moisture sorption

From the equilibrium values in the moisture uptake curves, information was extracted regarding the effect of plasticizer, plasticizer content and curing temperatures. Statistical analysis (ANOVA linear regression) of the data in Table 2 shows that there is a significant decrease in moisture content with increasing CA content for the non-cured and the 105 °C-cured samples. For the 150 °C cured samples, no trend was observed. The data for 50% RH were compared with the measurements performed on the films in the moisture chamber and the same trends were observed with both methods at all the different curing temperatures.

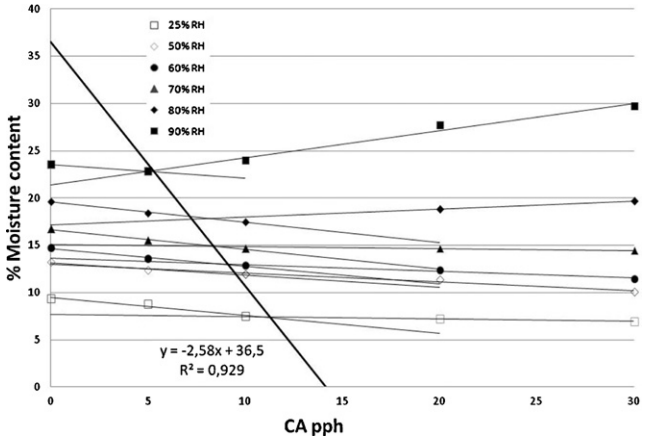

Fig. 1. Equilibrium moisture content at 23 °C in CA-plasticized films dried at 70 °C vs. amount of CA at different ambient RHs. The thick solid line (intersection line) indicates the boundary between single-phase and two-phase behavior.

In Fig. 1, the equilibrium moisture content at different relative humidities is shown as a function of CA content for TPS films dried at 70 °C without subsequent curing. Two different regions separated by an intersection line can be observed. To the left of the intersection line, there is a reduction in moisture uptake with increasing CA content. To the right, the decrease is smaller and, in fact, the moisture uptake increases with CA content above 70% RH. This indicates the presence of a two-phase system on the right-hand side with a starch-rich and a plasticizer-rich region, as previously reported elsewhere for GLY-plasticized TPS, where it was proposed that the intersection corresponded to monolayer coverage of the starch hydroxyl interaction sites (Godbillot et al., 2006). In such a model, the water is mainly adsorbed at interaction sites on the starch to the left of the intersection line. Whereas all the interaction sites on starch would theoretically be filled with plasticizer and water molecules on the right-hand side, so that additional water is mainly absorbed into the plasticizer-rich phase. The intersection with the x-axis indicates monolayer coverage of the plasticizer in the absence of water and the stoichiometric ratio of starch to GLY was 2 (Godbillot et al., 2006). From Fig. 1, it can be seen that monolayer coverage is reached at about 14 pph of CA. This corresponds to a ration between starch and CA of 8.5–1 which is significantly higher than for glycerol and which might be explained by the larger possibility for CA to form hydrogen bonds with the starch.

Fig. 2 shows the effect on the moisture sorption of subsequent curing at 105 °C. The same type of trend as in Fig. 1 suggesting an intersection line is also shown here. However, the subsequent curing affects the range in which phase separation occurs. The slope of the intersection line is reduced significantly and the point corresponding to CA monolayer coverage is shifted to a higher CA content than with the non-cured films. This change in slope may be explained by an esterification reaction between the CA and the starch. This reaction can theoretically lead to both monoester, diester and triester formation and can cross-link chains. The esterification of the starch by the CA reduces the amount of CA available to interact with the interaction sites of the starch, and it also means that some of the CA acts as an internal plasticizer and reduces the original hydroxyl interaction sites. It is also possible that cross-linking may lead to a more rigid open structure which can incorporate more of the plasticizer in between the starch chains. For the films cured at 105 °C,

Table 2
Moisture content for TPS with standard deviation for different CA-contents and curing temperatures stored in a climate room, 23 °C and 50% RH.

Curing temperature	% Moisture content				
	0 CA	5 CA	10 CA	20 CA	30 CA
Non-cured	12.57 ± 0.55	10.93 ± 0.39	10.17 ± 0.20	8.94 ± 0.67	7.99 ± 0.34
105 °C-cured	11.33 ± 0.65	10.31 ± 0.21	8.97 ± 0.05	8.39 ± 0.61	7.64 ± 0.39
150 °C-cured	10.75 ± 0.25	9.00 ± 0.65	8.56 ± 0.89	9.79 ± 0.10	8.64 ± 0.29

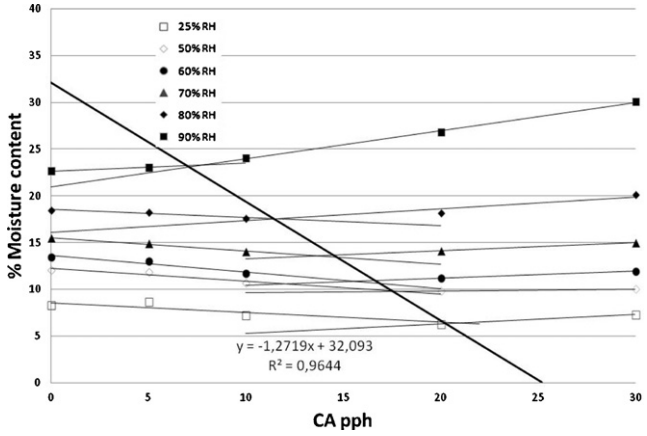

Fig. 2. Equilibrium moisture content at 23 °C in CA-plasticized film dried at 70 °C and cured at 105 °C vs. amount of CA at different ambient RHs. The thick solid line (intersection line) indicates the boundary between single-phase and two-phase behavior.

a significant decrease in the moisture content with increasing CA content occurs to the left of the intersection line up to 80% RH. To the right of the intersection line an increase in moisture content with increasing CA content is observed, but only the increase at 90% RH is significant. The explanations of this behavior have previously been discussed in detail for the non-cured samples in Fig. 1.

For the films dried at 70 °C and cured at 150 °C, there are no clear patterns (data not shown). This can be explained by a potential cross-linking reaction which would lead to a more rigid open structure and the loss of CA as an external plasticizer due to an esterification reaction between CA and the hydroxyl groups on the starch.

Fig. 3 shows the equilibrium moisture content of films with 30 pph CA at different curing conditions and the effect of different

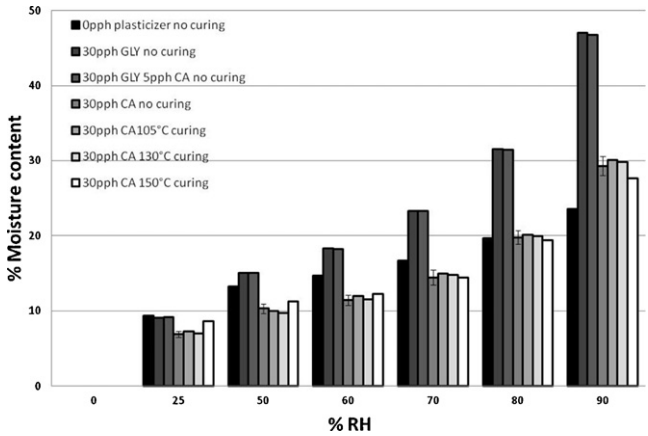

Fig. 3. Equilibrium moisture content at 23 °C for TPS with 30 pph CA at different curing temperatures and TPS with different plasticizers without subsequent curing vs. RH.

plasticizers without curing. It can clearly be seen that, for the films with 30 pph CA cured at ≤130 °C, there are only minor differences in the equilibrium moisture content which are not significant according to Student's *t*-test. For the film with 30 pph CA cured at 150 °C, there was a significant difference in the moisture uptake behavior compared to that at the lower curing temperatures. At low relative humidity, the 150 °C-cured film showed the highest moisture uptake but at high RH it showed the lowest uptake. This is an indication of cross-linking, which is known to reduce the swelling at high RH but to increase the moisture uptake at low RH (Larsson, Gimåker, & Wågberg, 2008). This originates from a rigid but more open structure with increasing cross-linking density. When the uncured films with high plasticizer content are compared with the unplasticized film dried at 70 °C, it is evident that GLY-plasticized TPS has a much higher moisture absorption than the CA-plasticized material over the entire RH range. The addition of 5 pph CA to TPS having 30 pph GLY did not significantly alter the moisture content compared to that of films plasticized with GLY alone. Compared to the unplasticized TPS, the CA-plasticized TPS showed a lower equilibrium moisture content up to almost 80% RH, whereas for the GLY-plasticized TPS the equilibrium moisture content was lower than that of the unplasticized TPS only up to between 25 and 50% RH. This is most probably explained by differences in the moisture uptake for the GLY rich and the CA rich phase. The result indicates that addition of CA can be used to reduce the moisture content of starch films up to higher % RH values than is possible with addition of glycerol.

3.3. Diffusion

The diffusion coefficients of the samples with different curing conditions were determined from the moisture uptake data by two different methods, each having their limitations, which are discussed below.

Method 1* (Eq. (5)) is based on the time to reach half the equilibrium uptake. In this method, it is assumed that the time to change the vapor pressure for each change in the target RH is infinitely small and that the surface has reached the equilibrium moisture content at the start of the experiment.

Method 2* (Eq. (6)) is based on the rate at which the film approaches equilibrium. This method is sensitive to small changes in weight close to equilibrium and uncertainties in the equilibrium moisture uptake, as can be seen in Eq. (6), especially when the logarithmic expression on the left-hand side of Eq. (6) approaches zero and the result approaches minus infinity. Thus, to minimize errors, the diffusion coefficient determination was performed at the range proposed elsewhere (Balik, 1996): $0.5 \leq (M_t/M_{eq}) \leq 0.8$.

The results from method 1* and method 2* should theoretically yield the same diffusion coefficient for a material in which the solute does not affect the diffusion coefficient (Crank, 1975). However, when the diffusion coefficient is dependent on the solute concentration, for instance when the solute acts as a plasticizer, method 2* is expected to yield a higher diffusion coefficient than method 1*, since the calculations are performed at a higher solute concentration.

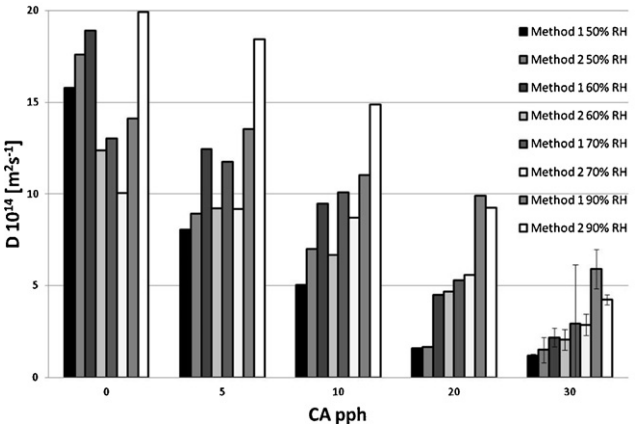

Fig. 4. Diffusion coefficient at 23 °C for TPS with different amount of CA dried at 70 °C without subsequent curing, calculated by method 1* and method 2* at different RHs.

3.4. Method evaluation

Fig. 4 shows the diffusion coefficients at 50%, 60%, 70% and 90% RH calculated by method 1* and method 2* for TPS films dried at 70 °C with different amount of CA without subsequent curing. First of all, an increased amount of CA leads to a reduction in the diffusion coefficient, regardless of the method used for evaluation. For samples with less than 10 pph CA there is a great difference between the diffusion coefficients derived by method 1* and method 2*. For 20 and 30 pph CA-plasticized films, however, the diffusion coefficient was almost the same by the two methods (up to 70% RH), but at higher RH, method 2* yielded a lower diffusion coefficient than method 1*. For 30 pph CA, Method 2* gives values with a fairly narrow confidence interval over the entire RH range, whereas method 1* shows a larger scatter. This difference between the methods is significant according to an *F*-test based on the in between group variation. This is probably due to the finite time taken to reach a new RH in the climate chamber during the measurements which affects method 1* more than method 2*. The trend toward a decreased diffusion coefficient at high moisture content, shown in Fig. 4 for films with 30 pph CA, obtained with both method 1* and method 2* is well documented in the literature and has been attributed to phenomena such as dual mode sorption (Masclaux, Goanvé, & Espuche, 2010), water clustering (Barrie & Platt, 1963) and polymer relaxation (Chivrac, Angellier-Coussy, Guillard, Pollet, & Averous, 2010; Vrentas & Duda, 1977; Vrentas, Jarzebski, & Duda, 1975). Another explanation could be a decrease in adsorption energy at high moisture contents (Fringant et al., 1996). However, the apparent decrease in the diffusion coefficient does not necessarily mean that the diffusion coefficient for water actually decreases, it can imply that the rate of mass transfer into the material is controlled by other mechanisms. Method 2* which is based on how fast the material approaches equilibrium is the more likely to be affected by slow changes in the material.

The comparison between the two diffusion coefficient calculation approaches highlights inherent weaknesses in the methods. The information in Fig. 4 can be used to highlight artifacts in the results and secondary mechanisms such as the high diffusion coefficient at low total plasticizer content and the decrease in the diffusion coefficient at high total plasticizer content. From these results, it is clearly seen that method 2* is more robust, which was shown with an *F*-test, showing a smaller variance at all relative humidities, but it may be less accurate at high total plasticizer content where mechanisms other than pure diffusion may influence the results. The diffusion coefficients presented in Table 3a–c and Fig. 5 are therefore based on method 2* for low- and intermediate total plasticizer contents. At the point where an increase in RH leads to a decrease in the diffusion coefficient at high RH, the diffusion coefficient is calculated by method 1*.

Table 3
(a) Diffusion coefficient at 23 °C for TPS dried at 70 °C without subsequent curing. (b) Diffusion coefficient at 23 °C for TPS dried at 70 °C and cured at 105 °C. (c) Diffusion coefficient at 23 °C for TPS dried at 70 °C and cured at 150 °C.

% RH	D ($\times 10^{14}$ m^2 s^{-1})						
	0 CA	5 CA	10 CA	20 CA	30 CA	30 GLY	5 CA 30 GLY
(a)							
50	17.6	8.91	7.01	1.65	1.18	11.8	11.8
60	12.4	9.22	6.66	4.66	2.33	18.7	19.3
70	10.0	9.17	8.70	5.56	3.12	20.7	21.3
80	13.3	15.4	14.9	12.3	10.6	16.6	17.5
90	19.9	18.5	14.9	9.92	6.16	6.12	7.10
(b)							
50	19.1	10.3	6.01	1.42	1.78	14.9	10.7
60	11.2	5.20	3.70	3.76	1.81	21.9	18.9
70	10.9	6.98	5.04	4.50	2.84	22.3	20.1
80	15.4	11.5	11.3	9.06	10.0	18.9	17.3
90	21.2	18.6	11.9	4.76	4.84	6.87	6.57
(c)							
50	14.8	10.5	5.12	0.76	2.03	13.6	10.5
60	10.1	6.86	5.09	2.43	2.94	19.8	17.9
70	8.34	6.59	4.70	4.19	3.48	21.4	19.8
80	13.7	11.4	12.8	8.34	6.76	18.1	16.8
90	20.8	17.8	12.9	4.05	6.43	6.76	6.57

Table 3a–c shows the diffusion coefficient of films with different plasticizers and different plasticizer content, dried at 70 °C at different curing temperatures. It is clearly seen that an increase in CA content significantly reduces the diffusion coefficient. GLY addition however gives a significant increase in the diffusion coefficient at 60–80% RH. A comparison for the diffusion coefficient at different curing temperatures shows that the films containing CA are significantly affected. For films with 20 pph CA, the diffusion coefficient decreases with increasing curing temperature. This is probably due to a reduction in molecular mobility due to cross-linking. This result suggests the onset of an esterification cross-linking reaction which would lead to a reduction in the amount of CA available to act as an external plasticizer.

Fig. 5 shows the relationship between diffusion coefficient and relative humidity for films with 20 pph and 30 pph CA and different curing conditions. The diffusion coefficient is strongly dependent on both the amount of CA and the curing conditions. It is clear that the material containing 20 pph CA without curing has a significantly higher diffusion coefficient over almost the entire RH range than all the other CA contents and curing conditions. At 20 pph CA, increasing the curing temperature reduced the diffusion coefficient over

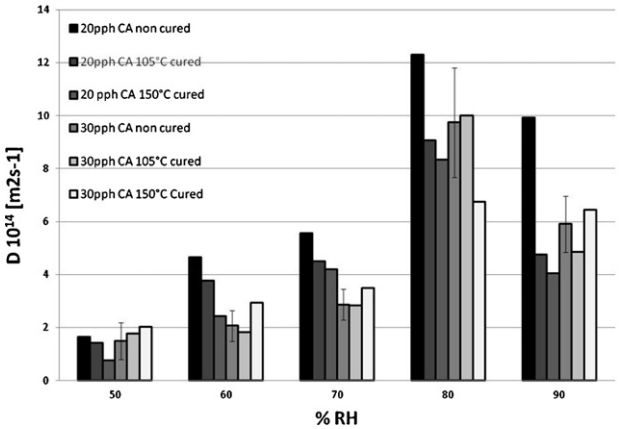

Fig. 5. Diffusion coefficient at 23 °C vs. relative humidity in TPS with 20 pph and 30 pph CA at different curing conditions.

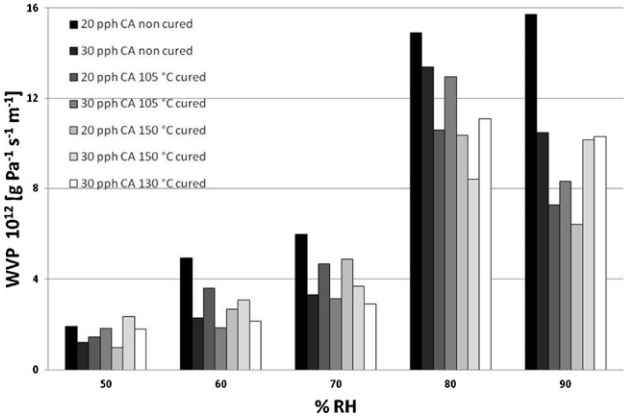

Fig. 6. WVP(Calc) at 23 °C for films with 20 pph and 30 pph CA with and without curing vs. RH.

the entire RH range. When the CA content was increased from 20 to 30 pph, a reduction of the diffusion coefficient at all curing temperatures was observed at 60 and 70% RH. Curing at 150 °C of the 30 pph CA films seemed to increase the diffusion coefficient up to 70% RH, but the diffusion coefficient decreased at 80% RH.

3.5. Permeability

Fig. 6 shows the WVP(Calc) (Eq. (8)) for TPS with 20 and 30 pph CA, the two recipes with the lowest diffusion coefficients and the lowest moisture sorption up to 70% RH being compared at different curing temperatures. It is clear that high-temperature curing affected the WVP of the TPS films and that this process can be used to lower WVP at high relative humidity as observed at 80% RH where an increase in curing temperature leads to a decrease in WVP for both 20 and 30 pph CA. This is probably due to cross-linking reactions which can influence both swelling and molecular movement. In these WVP data, it can be seen that with 20 and 30 pph CA, there was a decrease in WVP between 80% and 90% RH. This is due to the decreasing diffusion coefficient discussed previously in relation to Fig. 4, but it was not observed in the WVP(Dir) measurements presented in Table 4.

The WVP values calculated from the diffusion coefficient and solubility data and the WVP values obtained by direct measurement are of comparable magnitude as can be seen in Table 4. Since the direct measurements were performed with a gradient in relative humidity, instead of a constant RH for the diffusion and solubility measurements, the former method should theoretically yield significantly lower WVP values. The reason that this was not observed was probably due to an uneven thickness distribution of the coated samples due to penetration of the coating into the base paper and to defects in the coating such as cracks and pinholes. The diffusion and solubility data could therefore be used to assess the full potential of a "defect-free" coating.

Table 4
WVP from direct measurements (Dir) and calculated from diffusion and solubility data (calc).

% RH	WVP ($\times 10^{12}$ g Pa^{-1} s^{-1} m^{-1})	
	Dir	Calc
50	2.5	1.2
60	3.9	2.3
70	7.1	3.3
80	12	13
90	18	10

4. Conclusions

The addition of citric acid to TPS is a potential method to decrease both the moisture content and the diffusion coefficient and hence to improve the barrier properties, and this has been confirmed by water vapor permeability measurements. The diffusion coefficient decreased with increasing CA content for all curing conditions. The moisture content showed a more complex behavior due to a phase separation observed for non-cured and 105 °C cured films into regions of low and high CA content respectively, which may be separated by an intersection line in the graph. To the left of the intersection line, antiplasticization is thought to occur and in this region there was significant decrease in moisture content with increasing CA content. To the right of the intersection line, a two-phase system is thought to occur, and there were only minor differences in moisture content with increasing CA content up to 70% RH, followed by an increase in moisture content at higher RH. High-temperature (150 °C) curing seemed to have the greatest impact on diffusion coefficient and moisture sorption in the film with highest CA content. The moisture content of the film containing 30 pph CA cured at 150 °C was reduced at high % RH but increased at low and medium % RH. This could be explained by a cross-linking reaction leading to a rigid and more open structure that is less prone to swelling. Compared to TPS plasticized with glycerol, the addition of citric acid to TPS resulted in considerably lower diffusion coefficients and lower moisture content over the entire RH range.

Acknowledgements

The authors thank Ragnar Molander, StoraEnso, for fruitful discussions and StoraEnso for performing the moisture uptake measurements and permeability trials. This study was performed within the project Renewable Functional Barriers which is a part of the BFP research program, jointly launched by the Swedish Governmental Agency for Innovation Systems (VINNOVA), The Swedish Forest Industries Federation and *Trä-och Möbelföretagen* (TMF). The authors acknowledge VINNOVA and the industrial companies taking part in the project for financial support.

References

Andersson, C. (2008). New ways to enhance the functionality of paperboard by surface treatment – A review. *Packaging Technology and Science*, *21*(6), 339–373.
Angellier, H., Molina-Boisseau, S., Dole, P., & Dufresne, A. (2006). Thermoplastic starch – Waxy maize starch nanocrystals nanocomposites. *Biomacromolecules*, *7*(2), 531–539.
Averous, L., Fringant, C., & Moro, L. (2001). Plasticized starch–cellulose interactions in polysaccharide composites. *Polymer*, *42*(15), 6565–6572.
Balik, C. M. (1996). On the extraction of diffusion coefficients from gravimetric data for sorption of small molecules by polymer thin films. *Macromolecules*, *29*(8), 3025–3029.
Barrie, J. A., & Platt, B. (1963). The diffusion and clustering of water vapour in polymers. *Polymer*, *4*, 303–313.
Blanchard, E. J., Reinhardt, R. M., Graves, E. E., & Andrews, B. A. K. (1994). Dyeable cross-linked cellulose from low formaldehyde and non-formaldehyde finishing systems. *Industrial and Engineering Chemistry Research*, *33*(4), 1030–1034.
Cadogan, D. F., & Howick, C. J. (2008). Plasticizers. In *Ullmann's encyclopedia of industrial chemistry*. Weinheim: Wiley-VCH Verlag GmbH & Co. KGaA.
Carvalho, A. J. F., Zambon, M. D., Da Silva Curvelo, A. A., & Gandini, A. (2005). Thermoplastic starch modification during melt processing: Hydrolysis catalyzed by carboxylic acids. *Carbohydrate Polymers*, *62*(4), 387–390.
Chaudhary, D., & Adhikari, B. (2010). Effect of temperature and plasticizer molecular size on moisture diffusion of plasticized-starch biopolymer. *Starch-Stärke*, *62*(7), 364–372.
Chivrac, F., Angellier-Coussy, H., Guillard, V., Pollet, E., & Averous, L. (2010). How does water diffuse in starch/montmorillonite nano-biocomposite materials. *Carbohydrate Polymers*, *82*, 128–135.
Cho, S., Gällstedt, M., & Hedenqvist, M. S. (2010). Effects of glycerol content and film thickness on the properties of vital wheat gluten films cast at pH 4 and 11. *Journal of Applied Polymer Science*, *117*(6), 3506–3514.

Coma, V., Sebti, I., Pardon, P., Pichavant, F. H., & Deschamps, A. (2003). Film properties from crosslinking of cellulosic derivatives with a polyfunctional carboxylic acid. *Carbohydrate Polymers*, *51*(3), 265–271.

Crank, J. (1975). *The mathematics of diffusion* (2nd ed.). New York: Oxford University Press.

Deetae, P., Shobsngob, S., Varanyanond, W., Chinachoti, P., Naivikul, O., & Varavinit, S. (2008). Preparation, pasting properties and freeze–thaw stability of dual modified crosslink-phosphorylated rice starch. *Carbohydrate Polymers*, *73*(2), 351–358.

Forssell, P., Lahtinen, R., Lahelin, M., & Myllarinen, P. (2002). Oxygen permeability of amylose and amylopectin films. *Carbohydrate Polymers*, *47*(2), 125–129.

Fringant, C., Desbriéres, J., Milas, M., Rinaudo, M., Joly, C., & Escoubes, M. (1996). Characterisation of sorbed water molecules on neutral and ionic polysaccharides. *International Journal of Biological Macromolecules*, *18*, 281–286.

Gaspar, M., Benko, Z., Dogossy, G., Reczey, K., & Czigany, T. (2005). Reducing water absorption in compostable starch-based plastics. *Polymer Degradation and Stability*, *90*(3), 563–569.

Gaudin, S., Lourdin, D., Forssell, P. M., & Colonna, P. (2000). Antiplasticization and oxygen permeability of starch–sorbitol films. *Carbohydrate Polymers*, *43*(1), 33–37.

Gaudin, S., Lourdin, D., Le Botlan, D., Ilari, J. L., & Colonna, P. (1999). Plasticisation and mobility in starch–sorbitol films. *Journal of Cereal Science*, *29*(3), 273–284.

Godbillot, L., Dole, P., Joly, C., Roge, B., & Mathlouthi, M. (2006). Analysis of water binding in starch plasticized films. *Food Chemistry*, *96*(3), 380–386.

Habibi, Y., & Dufresne, A. (2008). Highly filled bionanocomposites from functionalized polysaccharide nanocrystals. *Biomacromolecules*, *9*(7), 1974–1980.

He, C., Hartmann, B., Lechner, M. D., Nierling, W., Seidel, C., & Kulicke, W. (2007). Influence of soluble polymer residues in crosslinked carboxymethyl starch on some physical properties of its hydrogels. *Starch-Stärke*, *59*(9), 423–429.

Hirashima, M., Takahashi, R., & Nishinari, K. (2004). Effects of citric acid on the viscoelasticity of cornstarch pastes. *Journal of Agricultural and Food Chemistry*, *52*(10), 2929–2933.

Huang, M., Yu, J., & Ma, X. (2006). High mechanical performance MMT-urea and formamide-plasticized thermoplastic cornstarch biodegradable nanocomposites. *Carbohydrate Polymers*, *63*(3), 393–399.

Jansson, A., & Jarnstrom, L. (2005). Barrier and mechanical properties of modified starches. *Cellulose*, *12*(4), 423–433.

Jiugao, Y., Ning, W., & Xiaofei, M. (2005). The effects of citric acid on the properties of thermoplastic starch plasticized by glycerol. *Starch-Stärke*, *57*(10), 494–504.

Jonhed, A., Andersson, C., & Jarnstrom, L. (2008). Effects of film forming and hydrophobic properties of starches on surface sized packaging paper. *Packaging Technology and Science*, *21*(3), 123–135.

Kalichevsky, M. T., & Blanshard, J. M. V. (1993). The effect of fructose and water on the glass transition of amylopectin. *Carbohydrate Polymers*, *20*(2), 107–113.

Larsson, P., Gimåker, M., & Wågberg, L. (2008). The influence of periodate oxidation on the moisture sorptivity and dimensional stability of paper. *Cellulose*, *15*(6), 837–847.

Lelievre, J. (1984). Effects of sugars on the swelling of crosslinked potato starch. *Journal of Colloid and Interface Science*, *101*(1), 225–232.

Lopez-Rubio, A., Lagaron, J. M., Ankerfors, M., Lindstrom, T., Nordqvist, D., Mattozzi, A., et al. (2007). Enhanced film forming and film properties of amylopectin using micro-fibrillated cellulose. *Carbohydrate Polymers*, *68*(4), 718–727.

Lourdin, D., Bizot, H., & Colonna, P. (1997). 'Antiplasticization' in starch-glycerol films? *Journal of Applied Polymer Science*, *63*(8), 1047–1053.

Lourdin, D., Coignard, L., Bizot, H., & Colonna, P. (1997). Influence of equilibrium relative humidity and plasticizer concentration on the water content and glass transition of starch materials. *Polymer*, *38*(21), 5401–5406.

Ma, X., Jian, R., Chang, P. R., & Yu, J. (2008). Fabrication and characterization of citric acid-modified starch nanoparticles/plasticized-starch composites. *Biomacromolecules*, *9*(11), 3314–3320.

Magalhães, N. F., & Andrade, C. T. (2009). Thermoplastic corn starch/clay hybrids: Effect of clay type and content on physical properties. *Carbohydrate Polymers*, *75*(4), 712–718.

Mali, S., Sakanaka, L. S., Yamashita, F., & Grossmann, M. V. E. (2005). Water sorption and mechanical properties of cassava starch films and their relation to plasticizing effect. *Carbohydrate Polymers*, *60*(3), 283–289.

Masclaux, C., Goanvé, F., & Espuche, E. (2010). Experimental and modelling studies of transport in starch nanocomposite films as affected by relative humidity. *Journal of Membrane Science*, *363*, 221–231.

Mathew, A. P., & Dufresne, A. (2002). Plasticized waxy maize starch: Effect of polyols and relative humidity on material properties. *Biomacromolecules*, *3*(5), 1101–1108.

Moller, H., Grelier, S., Pardon, P., & Coma, V. (2004). Antimicrobial and physicochemical properties of chitosan-HPMC-based films. *Journal of Agricultural and Food Chemistry*, *52*(21), 6585–6591.

Ning, W., Xingxiang, Z., Na, H., & Jianming, F. (2010). Effects of water on the properties of thermoplastic starch poly(lactic acid) blend containing citric acid. *Journal of Thermoplastic Composite Materials*, *23*(1), 19–34.

Park, H., Lee, W., Park, C., Cho, W., & Ha, C. (2003). Environmentally friendly polymer hybrids Part I mechanical, thermal, and barrier properties of thermoplastic starch/clay nanocomposites. *Journal of Materials Science*, *38*(5), 909–915.

Reddy, N., & Yang, Y. (2010). Citric acid cross-linking of starch films. *Food Chemistry*, *118*(3), 702–711.

Rutenberg, M. W., & Solarek, D. (1984). Starch derivates: Properties and uses. In R. L. Whistler, J. N. Bemiller, & E. F. Pachall (Eds.), *Starch: Chemistry and technology* (2nd ed., pp. 312–388). Orlando, FL, USA: Academic Press Inc.

Seidel, C., Kulicke, W., Hess, C., Hartmann, B., Lechner, M. D., & Lazik, W. (2001). Influence of the cross-linking agent on the gel structure of starch derivatives. *Starch-Stärke*, *53*(7), 305–310.

Shi, R., Bi, J., Zhang, Z., Zhu, A., Chen, D., Zhou, X., et al. (2008). The effect of citric acid on the structural properties and cytotoxicity of the polyvinyl alcohol/starch films when molding at high temperature. *Carbohydrate Polymers*, *74*(4), 763–770.

Shi, R., Zhang, Z., Liu, Q., Han, Y., Zhang, L., Chen, D., et al. (2007). Characterization of citric acid/glycerol co-plasticized thermoplastic starch prepared by melt blending. *Carbohydrate Polymers*, *69*(4), 748–755.

Shogren, R. L., Lawton, J. W., Tiefenbacher, K. F., & Chen, L. (1998). Starch–poly(vinyl alcohol) foamed articles prepared by a baking process. *Journal of Applied Polymer Science*, *68*(13), 2129–2140.

Stading, M., Rindlav-Westling, A., & Gatenholm, P. (2001). Humidity-induced structural transitions in amylose and amylopectin films. *Carbohydrate Polymers*, *45*(3), 209–217.

Svagan, A. J., Hedenqvist, M. S., & Berglund, L. (2009). Reduced water vapour sorption in cellulose nanocomposites with starch matrix. *Composites Science and Technology*, *69*(3–4), 500–506.

Talja, R., & Poppius-Levlin, K., 2010. Xylan from wood biorefinery – A novel approach. Presented at the FlexPakRenew Workshop, 2010-05-10 Lyon France, 10052010 2010.

Vrentas, J. S., & Duda, J. L. (1977). Diffusion in polymer? Solvent systems. III. Construction of Deborah number diagrams. *Journal of Polymer Science: Polymer Physics Edition*, *15*(3), 441–453.

Vrentas, J. S., Jarzebski, C. M., & Duda, J. L. (1975). A Deborah number for diffusion in polymer–solvent systems. *AIChE Journal*, *21*(5), 894–901.

Wang, Y., & Wang, L. (2000). Effects of modification sequence on structures and properties of hydroxypropylated and crosslinked waxy maize starch. *Starch-Stärke*, *52*(11), 406–412.

Wing, R. E. (1996). Starch citrate: Preparation and ion exchange properties. *Starch-Stärke*, *48*(7–8), 275–279.

Wurzburg, O. B. (1986). Cross-linked starches. In O. B. Wurzburg (Ed.), *Modified starch properties and uses* (pp. 41–53). Boca Raton, FL: CRC Press, Inc.

Xie, X., & Liu, Q. (2004). Development and physicochemical characterization of new resistant citrate starch from different corn starches. *Starch-Stärke*, *56*(8), 364–370.

Yoon, S., Chough, S., & Park, H. (2006). Properties of starch-based blend films using citric acid as additive. II. *Journal of Applied Polymer Science*, *100*(3), 2554–2560.

Yu, J., Chang, P. R., & Ma, X. (2010). The preparation and properties of dialdehyde starch and thermoplastic dialdehyde starch. *Carbohydrate Polymers*, *79*(2), 296–300.